LIMNOLOGY
and
OCEANOGRAPHY: METHODS

ASLO

Limnol. Oceanogr.: Methods 2022

doi: 10.1002/lom3.10486

Accurate spectrophotometric pH measurements made directly in the sample bottle using an aggregated dye perturbation approach

Yuichiro Takeshita,[1]* **Keaton L. Mertz**,[2] **Addie Norgaard**,[3] **Sara Gray**,[3] **Maddie H. Verburg**,[3] **Emily E. Bockmon**[3]

[1]Monterey Bay Aquarium Research Institute, Moss Landing, California, USA
[2]Department of Chemistry, University of Wisconsin Madison, Madison, Wisconsin, USA
[3]Department of Chemistry and Biochemistry, California Polytechnic State University, San Luis Obispo, California, USA

Abstract

Spectrophotometric pH measurements of seawater (pH_{spec}) are routinely made by the oceanographic community for a wide variety of studies. However, obtaining consistent measurements between laboratories that meet stringent thresholds such as the "weather" (± 0.02) and "climate" (± 0.003) standards, has been a challenge. One of the main sources of error for pH_{spec} measurements is gas exchange of carbon dioxide during sample handling. Here, we present a simple method where pH_{spec} measurements on the total scale are made directly in the sampling bottle, which minimizes sample handling errors because the solution is not transferred during analysis. We compared the performance of this method to a standard automated benchtop system on a hydrography cruise, and the two methods were consistent to 0.003 ± 0.0033 (1σ). This demonstrates that this simple method can produce pH_{spec} that approaches climate quality, and comfortably meets weather quality standards. Additional benefits include high sample throughput, and the ability to rapidly quantify dye perturbation effects for each sample. The latter should be particularly useful for low salinity samples such as those taken from estuaries, insofar as modifications specific to the pH_{spec} measurements of estuarine waters are employed.

Seawater pH is measured to track the progression of ocean acidification (Byrne et al. 2010), understand ecosystem health and dynamics (Hofmann et al. 2011; Challener et al. 2016; Takeshita et al. 2016; Chan et al. 2017; Silbiger and Sorte 2018), and can be used to calculate additional carbonate system parameters such as the partial pressure of carbon dioxide (Williams et al. 2017; Takeshita et al. 2018) and calcium carbonate saturation state (Harris et al. 2013; Takeshita et al. 2015; Feely et al. 2016). It is also routinely measured for ocean acidification studies to validate control and experimental conditions (Riebesell et al. 2010; Bockmon et al. 2013; Galloway et al. 2020), and can be used for estuarine samples (Müller et al. 2018). Therefore, the ability to make consistent and accurate pH measurements is important for a wide variety of applications throughout the marine science community.

Spectrophotometric measurements using sulfenophthalein indicator dyes are the standard for seawater pH measurements (pH_{spec}), due to their high levels of precision and reproducibility (Clayton and Byrne 1993; Dickson et al. 2007; Rérolle et al. 2012; Ma et al. 2019). The most commonly used indicator dye is meta-cresol purple (mCP), because its pK_A is near nominal seawater pH. Significant improvements in accuracy were achieved when impurities from mCP were removed (Liu et al. 2011; Patsavas et al. 2013; DeGrandpre et al. 2014). Furthermore, development of automated benchtop systems has improved repeatability of pH_{spec} (Carter et al. 2013), and are now being used for many repeat hydrography cruises (Álvarez et al. 2020).

The Global Ocean Acidification Observation Network (GOA-ON) has defined thresholds for uncertainties of pH measurements used to study different types of processes (Newton et al. 2015). Climate quality pH measurements are sufficient to study long term, multi-decadal climate driven changes in ocean pH due to ocean acidification, and should have an uncertainty of ± 0.003. On the other hand, weather quality pH measurements are sufficient to study more dynamic processes such as phytoplankton blooms and upwelling that occur on shorter timescales, and should have a maximum uncertainty of ± 0.02. Recently, pH_{spec} measurements

*Correspondence: yui@mbari.org

Additional Supporting Information may be found in the online version of this article.

consistent to ± 0.003 (range) were achieved between four laboratories with high levels of expertise using purified mCP, demonstrating that climate-level consistency can be achieved when sophisticated instrumentation is operated by experts (Takeshita et al. 2021b).

However, obtaining consistent pH measurements across the oceanographic community among laboratories with scientists and managers with varying levels of experience and expertise to meet climate, and in many cases weather quality measurements, has been a challenge. For example, an interlaboratory study that included 26 different laboratories around the world (Bockmon and Dickson 2015) demonstrated that pH_{spec} measurements of a certified reference material (CRM) with pH 7.88 had a range of ± 0.04. The consistency was worse at lower pH (7.55), and skewed toward higher pH values. Based on this observation, they concluded that a major contributor to this variability was carbon dioxide (CO_2) loss due to sample handling during analysis. Thus, improvements or modifications in analytical methods that minimizes sample handling should lead to more accurate and consistent pH_{spec} measurements across the community.

Here, we present a simple method for measuring pH_{spec} where absorbance measurements are made using the sample bottle as the cell, and demonstrate that it has comparable performance with a standard, automated benchtop system (Carter et al. 2013). We refer to this method as "spec in a bottle" (SIAB), and it has several advantages, such as minimizing errors due to sample handling and high sample throughput. We compared the performance of the SIAB method to the standard approach on a hydrography cruise off the central coast of California, and demonstrate similar performance between the two. Finally, it is straightforward to correct for dye perturbation effects, which can be useful for achieving accurate pH measurements in low salinity or low buffered samples such as those from estuaries.

Materials and methods

A picture of the SIAB setup is shown in Fig. 1. A 250-mL borosilicate glass media bottle (Pyrex; McMaster 4787T62) was used for the sampling bottle and spectrophotometric cell, and was held in place in the light path by a custom 3-D printed cell holder. The cell path length is ∼ 7 cm, and an Agilent 8453 spectrophotometer was used to make absorbance measurements. The solution was stirred with a stir bar, using a stir plate created by gluing two magnets to a computer fan which was secured to the bottom of the cell holder. Dye was injected into the bottle using a 50-μL solenoid pump (Lee, LPL series) through an opaque 1/16'' PEEK tubing to prevent dye from degrading due to light exposure. Temperature of the solution was measured using a NIST traceable thermometer (QTI DTU6028-002), with an accuracy of ± 0.02°C. A cap was lightly screwed on the bottle during analysis to minimize gas exchange. The thermometer and dye injection tubing were

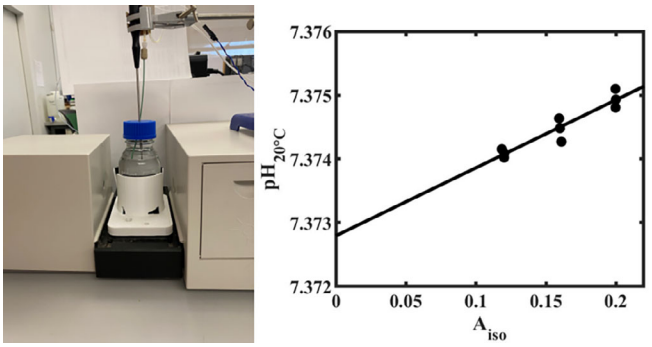

Fig. 1. (Left) Picture of the spec in a bottle setup. (Right) Typical results from this approach show pH calculations from three dye additions each measured in triplicate. The intercept gives the pH of the original sample before dye is added.

inserted through a small hole in the cap. The system was controlled using a custom LabVIEW program, and the stir plate and solenoid pump was actuated using a MOSFET controlled by an Arduino. Files necessary to replicate this system is provided in the supplementary materials.

For analysis, the sampling bottle was wiped clean using a Kimwipe, and placed securely into the cell holder while ensuring that the seam of the bottle was not in the light path. A cap with the thermometer and dye inlet was secured onto the bottle, and the sample was stirred for 60 s. Then three blank spectra were collected, and averaged. This was followed by three injections of dye, with the first injection being the largest so that the absorbance at the isosbestic wavelength (A_{iso}; 487 nm) was ∼ 0.1, and the final A_{iso} was ∼ 0.20 (Fig. 1). For a 10 mM dye solution, the additions were ∼ 150, 50, and 50 μL. The sample was stirred for 30 s after each dye addition, and three absorbance spectra and temperature measurements were collected and averaged after each addition. The solution was not stirred while making absorbance measurements. The whole process took ∼ 3.5 min.

The pH of the original sample before dye addition was calculated as the y-intercept from a least-squares linear regression between pH measured after each dye addition vs. A_{iso} (Fig. 1). All pH is reported on the total scale. Each pH measurement was corrected to a constant temperature (in this case 20°C) prior to conducting the linear regression, as this minimizes any biases that may arise from temperature changes during analysis. For example, if the sample temperature was substantially different than room temperature ($|\Delta T| > 4$°C), sample temperature typically changed by a couple tenths of a degree during analysis. Furthermore, pH_{spec} is typically reported at a constant temperature (e.g., 20°C or 25°C). CO2SYS was used to correct pH to 20°C (van Heuven et al. 2011) with total alkalinity (TA) as the second input. The temperature dependence of seawater pH ($\Delta pH/\Delta T$) is not particularly sensitive to TA, thus, a general estimate of TA through regional S-TA relationships or global algorithms (Bittig et al. 2018; Carter et al. 2018) for open or coastal oceans with minimal

freshwater influence should be sufficient. We note that such a relationship will not be applicable for estuarine samples (Jiang et al. 2014), thus, an independent measurement or estimate of TA of the sample would be required. See Discussion for more details.

We assessed the performance of this approach on the Central California Coast pH and Oxygen (C3PO) cruise in 2019 (Takeshita et al. 2021a). pH measurements were made on samples collected from 1000 m to the surface off the coast of Central California, up to 250 km offshore ($n = 91$). Seawater samples were collected into the media bottles following standard protocols (Dickson et al. 2007), and analyzed within 4 h of collection. Since samples were run soon after collection, they were not poisoned. Duplicate samples were taken to assess overall precision, which was estimated to be ± 0.002 (1σ; $n = 7$). Samples were placed in a water bath for at least 1 h to raise the sample temperature to near room temperature. Approximately 30 different media bottles were used for this analysis, demonstrating good bottle to bottle reproducibility. Samples drawn from the same Niskin bottles were analyzed for pH using a standard benchtop system based on the design of Carter et al. 2013. This design has been demonstrated to be robust, and is utilized on repeat hydrography cruises (Feely et al. 2016; Álvarez et al. 2020) as well as for the standard pH measurement for the CRM intercomparison study (Bockmon and Dickson 2015). Purified meta-Cresol Purple dye was used for both systems (Liu et al. 2011), and dye was adjusted to pH ~ 7.8 in 0.7 M NaCl background. Sample salinity ranged between 33.11 and 34.47.

In addition to correcting dye perturbation for each sample as described above, dye perturbation effects were corrected for using an aggregated approach, where an average dye perturbation relationship was obtained from measurements made throughout the cruise, and applied to the pH measurement after the third addition of dye (Fig. 2). Note that the dye perturbation slope is normalized to A_{iso}, thus, the actual magnitude of the correction is approximately a fifth of what is plotted. Such an aggregated correction has been successfully applied for standard pH_{spec} measurements previously (Clayton and Byrne 1993; Carter et al. 2013).

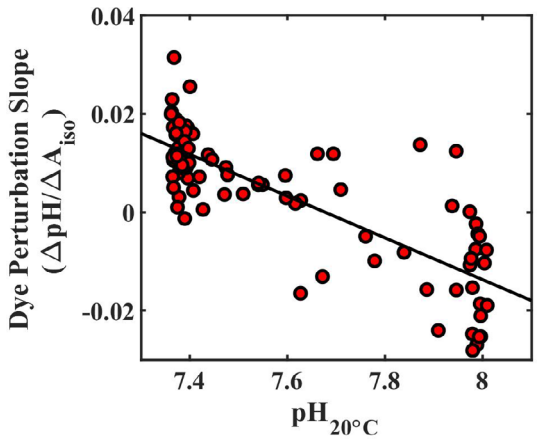

Fig. 2. Dye perturbation slope ($\Delta pH/\Delta A_{iso}$) obtained from each sample from the cruise ($n = 91$). Black line is a linear regression through the data (-0.042 (± 0.003 SE) $\times$ pH $+ 0.326$ (± 0.026 SE)), and represents the aggregated dye perturbation relationship.

Assessment

There was good agreement between pH_{SIAB} and $pH_{standard}$ from the cruise on average, with a mean difference of 0.003 ± 0.0033 (1σ) when dye perturbation was corrected for each sample individually (black triangles, Fig. 3). Slightly better agreement and reproducibility was observed with the aggregated dye perturbation correction approach (red circles, Fig. 3), with a mean difference of 0.002 ± 0.0023 (1σ). The difference was mainly driven by samples at higher pH (> 7.9), where reproducibility was noticeably worse when dye perturbation corrections were applied to each sample (± 0.004; 1 σ) compared to those using the aggregated approach (± 0.002; 1 σ). This is also reflected in the higher variability of the dye perturbation slopes at higher pH (± 0.006 at pH ~ 7.4 vs. ± 0.011 at pH ~ 8) (Fig. 2). The mean difference between the two methods had a slight solution pH dependence, where agreement was slightly better at pH ≈ 7.4 (0.002) compared to pH ≈ 8 (0.004). However, these slight differences in the mean could have been caused by biases in the dye perturbation correction due to larger variability at higher pH. Alternatively, it could reflect real changes in sample pH due to biological activity prior to analysis, as pH samples were not poisoned. Nonetheless, these results demonstrate that pH measurements that are consistent to the standard method to ± 0.01 (range), and for the majority of the time to better than ± 0.005, can be obtained using this approach regardless of the method used for dye perturbation correction. While this comes close to meeting climate quality standards, it comfortably meets weather quality pH measurements, and thus should be useful for a variety of applications.

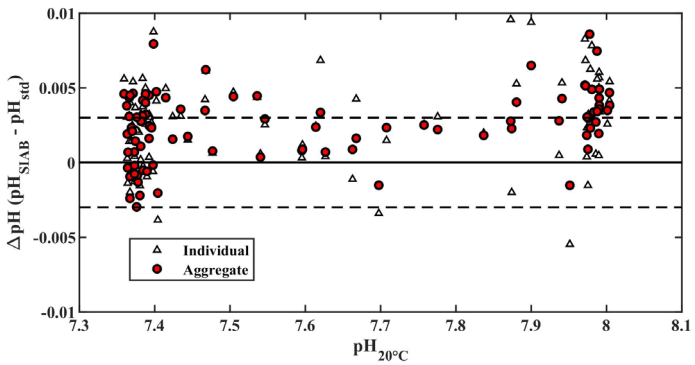

Fig. 3. Difference in pH ($pH_{SIAB} - pH_{standard}$) vs. sample pH ($n = 91$) from the C3PO cruise. Solid line represents 0, and dashed line represents the climate quality threshold of ± 0.003.

Discussion

There are several potential causes for the observed larger uncertainty in dye perturbation correction at higher pH. First, the uncertainty of the calculated dye perturbation slope and intercept will be larger when solution pH is similar to dye pH, as the magnitude of the dye perturbation is similar to the instrumental precision. Dye pH was adjusted to ~ 7.8 for this study, thus could explain why reproducibility was slightly worse around this pH. Second, the precision of the pH measurements also became slightly worse with higher solution pH (Fig. 4). The precision was calculated as the standard deviation of pH from the triplicate absorbance measurements made after each dye addition. Reduced precision would lead to larger uncertainties for the linear regression, thus, higher uncertainty in the final calculated pH. The reduced precision could have been caused by particles in the samples, as the higher pH samples were near surface samples and this cruise was in productive waters off the coast of California. Filtering samples prior to analysis may improve reproducibility at higher pH (Bockmon and Dickson 2014). Therefore if samples are nominal seawater (i.e., similar TA), then we recommend using the aggregated dye perturbation approach if possible, to produce more reproducible pH values. This will also lead to shorter analysis time, as only a single injection of dye is required.

A critical step for achieving accurate pH measurements for this approach is to correct the pH measured at the solution temperature to a reference temperature such as 20°C or 25°C. This requires knowing, or at least reasonably estimating, a second parameter such as TA. The temperature sensitivity of sample pH (ΔpH/ΔT) varies depending on its DIC and TA, although this term is not particularly sensitive to errors in input TA in most cases (Fig. 5). The ΔpH/ΔT is most sensitive to uncertainties in TA when TA is equal to DIC. However, when TA is above 1500 μmol kg^{-1}, a bias of 50 μmol kg^{-1} in TA would lead to an error in |ΔpH/ΔT| of <0.0025 in the worst case scenario (i.e., when DIC = TA). When TA is 400 μmol kg^{-1}, the same bias in TA would lead to an error in |ΔpH/ΔT| of <0.005. Global (Bittig et al. 2018; Carter et al. 2018) or regional algorithms (Alin et al. 2012; Takeshita et al. 2015; Hirsh et al. 2020; Wright-Fairbanks et al. 2020) that estimate TA from temperature and salinity have sufficient accuracy to constrain TA for the open ocean, so this source of temperature dependent error becomes negligible. Direct measurements for TA will likely be needed for environments with large freshwater influence such as estuaries or go through large biological modification from calcification such as on coral reefs. This error can also be minimized by analyzing samples near the target temperature, for example by pre-equilibrating the bottle temperature in a water bath prior to analysis. On our cruise, there was no discernable trend in the residual between pH_{SIAB} and $pH_{standard}$ when sample temperature was within ± 3°C of 20°C. This suggests that this source of error is negligible as long as sample temperature is within 3°C of the temperature at which pH is reported.

There are several additional advantages for this approach. First, it minimizes potential errors due to loss of CO_2 during sample handling. A pH intercomparison study revealed that sample handling was likely the dominant source of error of pH measurements for most laboratories conducting spectrophotometric pH measurements (Bockmon and Dickson 2015). The source of this error could be as large as ± 0.04. Therefore, removing this source of error would lead to significant improvements in the quality of pH measurements by the community. While it is possible to avoid this source of error, it typically requires specialized equipment and high levels of expertise (Carter et al. 2013). The spec in a bottle offers a simple and affordable solution to minimize this source of error. Second, this approach allows a high sample throughput, as sample analysis only takes several minutes. This could be beneficial for intensive field campaigns or during mesocosm studies where routine pH measurements of control and experimental tanks would be beneficial (Galloway et al. 2020).

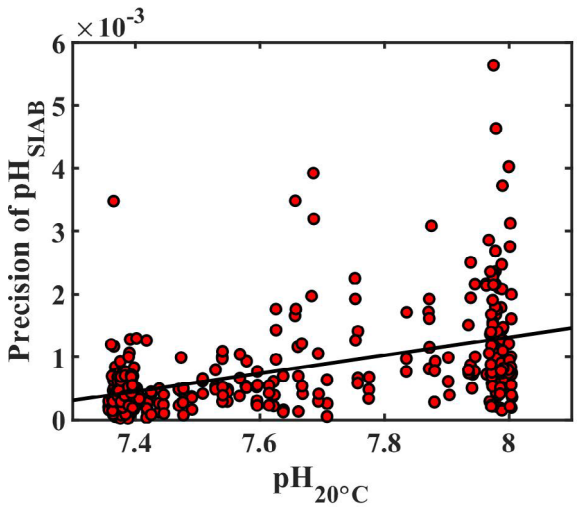

Fig. 4. Precision of pH measurements vs. solution pH.

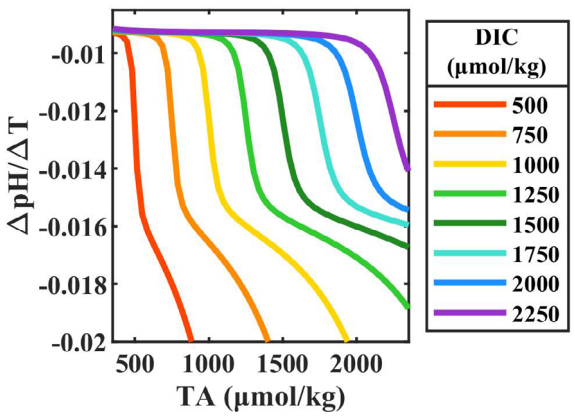

Fig. 5. ΔpH/ΔT at 20°C vs. TA. Contours represent DIC (μmol kg^{-1}).

The ability to readily conduct multiple dye additions should also be beneficial for laboratories that routinely run samples that span a large range in salinity (thus also TA), such as from estuaries. However, it is noted that additional care must be taken for pH_{spec} measurements on estuarine samples, particularly if there are very high concentrations of dissolved organic matter, hydrogen sulfide, or colored materials in the sample (Müller et al. 2018). Such precautions would apply to the SIAB approach as well. Typically, the magnitude of the perturbation is greater at lower salinity, thus correcting for the perturbation is even more important for obtaining accurate sample pH (Yuan and Degrandpre 2008; Li et al. 2020). An aggregated approach for dye perturbation correction is not practical for samples spanning a large range of salinity, as the perturbation slope would need to be characterized for multiple salinities and/or TA. Thus, for such samples, correcting dye perturbation effects on individual samples may be more appropriate. Furthermore, it will be beneficial for the dye solution to have similar ionic strength as the sample to minimize changes in salinity during analysis, as this affects the calculated pH through the salinity dependent thermodynamic terms. This may not be logistically practical when samples have a large salinity range, but its effect can be corrected for by applying a dilution calculation if the sample salinity is known. It is noted that small changes in salinity has a larger effect on calculated pH at low salinities than at high salinities (Mosley et al. 2004; Müller and Rehder 2018), thus, preparing dye solutions with ionic strength that more closely match the lower salinity samples would further minimize this error. A limitation for this approach is the amount of dye that is used for each analysis due to the relatively large sample volume required, as it uses approximately five times more dye per sample than the standard approach utilizing a 10-cm cell. This is because enough dye must be added to the whole sample volume rather than just for the cuvette to reach the target absorbances (i.e., target dye concentration in the sample solution), as typically done. The amount of dye required is dependent on cell length and sample volume (Chierici et al. 1999). This can get prohibitively expensive when using purified mCP. However, unpurified mCP dye is affordable, thus should not represent a substantial increase in cost. Accurate pH measurements can still be obtained using unpurified mCP by following published protocols (Liu et al. 2011; Douglas and Byrne 2017). The amount of required dye can likely be reduced by utilizing a smaller bottle. However, if the bottle is too small, the curvature in the glass may lead to increased refraction of the light and lead to errors in the measured pH. This could potentially be alleviated by using square bottles. Careful investigation into these effects should be conducted prior to utilizing smaller bottles.

Comments and recommendations

The media bottles utilized in this study are not suitable for long-term storage, so this method should be used for on-site analysis, or very short term storage (< 1 week). Even for short-term storage, care should be taken to thoroughly dry the sealing surfaces to minimize gas exchange during storage. We also found it helpful to reject bottles that produced noticeably noisy absorbance spectra for the blank solutions, which was ~ 5% of bottles. The bottles should also be stored and transported carefully to avoid damaging the glass, as scratches will lead to noisy absorbance and pH measurements. Finally, it is unclear whether similar performances could be achieved from other glass types such as soda lime, thus, careful assessment should be conducted prior to utilizing such bottles.

This approach should be readily adaptable for spectrophotometric systems utilizing fiber optics as well. For example, (Liu et al. 2015) measured pH using Biochemical Oxygen Demand borosilicate bottles with a fiber-optic based spectrophotometric system (Ocean Optics USB4000). While their study does not report the reproducibility of pH measurements, they obtained very precise TA measurements (< 1 μmol kg^{-1}), suggesting high reproducibility for pH measurements as well. However, it is unclear if the same accuracy of measurements can be achieved with these fiber-optic based spectrometers. For example, accuracy of pH measurements is dependent on the spectral bandwidth resolution of the spectrometer (DeGrandpre et al. 2014). However, such biases would result from the quality of the spectrometer rather than using the bottle as the spectrophotometric cell. Furthermore, fiber optic-based systems will likely be more susceptible for stray light contamination, thus, additional care may be necessary to prevent room light from entering the spectrometer.

Data availability statement

Data used in this study are included in the Supporting Information Material S1, and cruise data can be found at the National Center for Environmental Information, accession number 0225432.

References

Alin, S. R., R. A. Feely, A. G. Dickson, J. M. Hernández-Ayón, L. W. Juranek, M. D. Ohman, and R. Goericke. 2012. Robust empirical relationships for estimating the carbonate system in the southern California Current System and application to CalCOFI hydrographic cruise data (2005–2011). J. Geophys. Res. **117**: C05033. doi:10.1029/2011JC007511

Álvarez, M., N. M. Fajar, B. R. Carter, E. F. Guallart, F. F. Pérez, R. J. Woosley, and A. Murata. 2020. Global ocean spectrophotometric pH assessment: Consistent inconsistencies. Environ. Sci. Technol. **54**: 10977–10988. doi:10.1021/acs.est.9b06932

Bittig, H. C., T. Steinhoff, H. Claustre, B. Fiedler, N. L. Williams, R. Sauzède, A. Körtzinger, and J.-P. Gattuso. 2018. An alternative to static climatologies: Robust estimation of open ocean CO2 variables and nutrient

concentrations from T, S, and O2 data using Bayesian neural networks. Front. Mar. Sci. **5**: 328. doi:10.3389/fmars.2018.00328

Bockmon, E. E., and A. G. Dickson. 2014. A seawater filtration method suitable for total dissolved inorganic carbon and pH analyses. Limnol. Oceanogr. Methods **12**: 191–195. doi:10.4319/lom.2014.12.191

Bockmon, E. E., and A. G. Dickson. 2015. An inter-laboratory comparison assessing the quality of seawater carbon dioxide measurements. Mar. Chem. **171**: 36–43. doi:10.1016/j.marchem.2015.02.002

Bockmon, E. E., C. A. Frieder, M. O. Navarro, L. A. White-Kershek, and A. G. Dickson. 2013. Technical note: Controlled experimental aquarium system for multi-stressor investigation of carbonate chemistry, oxygen saturation, and temperature. Biogeosciences **10**: 5967–5975. doi:10.5194/bg-10-5967-2013

Byrne, R. H., S. Mecking, R. A. Feely, and X. Liu. 2010. Direct observations of basin-wide acidification of the North Pacific Ocean. Geophys. Res. Lett. **37**: 1–5. doi:10.1029/2009GL040999

Carter, B. R., R. A. Feely, N. L. Williams, A. G. Dickson, M. B. Fong, and Y. Takeshita. 2018. Updated methods for global locally interpolated estimation of alkalinity, pH, and nitrate. Limnol. Oceanogr. Methods **16**: 119–131. doi:10.1002/lom3.10232

Carter, B. R., J. A. Radich, H. L. Doyle, and A. G. Dickson. 2013. An automated system for spectrophotometric seawater pH measurements. Limnol. Oceanogr. Methods **11**: 16–27. doi:10.4319/lom.2013.11.16

Challener, R. C., L. L. Robbins, and J. B. Mcclintock. 2016. Variability of the carbonate chemistry in a shallow, seagrass-dominated ecosystem: Implications for ocean acidification experiments. Mar. Freshw. Res. **67**: 163–172. doi:10.1071/MF14219

Chan, F., and and others. 2017. Persistent spatial structuring of coastal ocean acidification in the California Current System. Sci. Rep. **7**: 2526. doi:10.1038/s41598-017-02777-y

Chierici, M., A. Fransson, and L. G. Anderson. 1999. Influence of m-cresol purple indicator additions on the pH of seawater samples: Correction factors evaluated from a chemical speciation model. Marine Chemistry **65**: 281–290. doi:10.1016/S0304-4203(99)00020-1

Clayton, T. D., and R. H. Byrne. 1993. Spectrophotometric seawater pH measurements: Total hydrogen ion concentration scale calibration of m-cresol purple and at-sea results. Deep Sea Res Part I. Oceanogr. Res. Pap. **40**: 2115–2129. doi:10.1016/0967-0637(93)90048-8

DeGrandpre, M. D., R. S. Spaulding, J. O. Newton, E. J. Jaqueth, S. E. Hamblock, A. A. Umansky, and K. E. Harris. 2014. Considerations for the measurement of spectrophotometric pH for ocean acidification and other studies. Limnol. Oceanogr. Methods **12**: 830–839. doi:10.4319/lom.2014.12.830

Dickson, A. G., C. L. Sabine, and J. R. Christian [eds.]. 2007. Guide to best practices for ocean CO2 measurements. North Pacific Marine Science Organization. doi:10.25607/OBP-1342

Douglas, N. K., and R. H. Byrne. 2017. Achieving accurate spectrophotometric pH measurements using unpurified meta-cresol purple. Mar. Chem. **190**: 66–72. doi:10.1016/j.marchem.2017.02.004

Feely, R. A., and and others. 2016. Chemical and biological impacts of ocean acidification along the west coast of North America. Estuar. Coast. Shelf Sci. **183**: 260–270. doi:10.1016/j.ecss.2016.08.043

Galloway, A. W. E., and and others. 2020. Ghost factors of laboratory carbonate chemistry are haunting our experiments. Biol. Bull. **239**: 183–188. doi:10.1086/711242

Harris, K. E., M. D. DeGrandpre, and B. Hales. 2013. Aragonite saturation state dynamics in a coastal upwelling zone. Geophys. Res. Lett. **40**: 2720–2725. doi:10.1002/grl.50460

van Heuven, S., D. Pierrot, J. W. B. Rae, E. Lewis, and D. W. Wallace. 2011. MATLAB program developed for CO2 system calculations. ORNL/CDIAC-105b, Carbon Dioxide Information Analysis Center, Oak Ridge National Laboratory, U.S. Department of Energy, Oak Ridge, TN. doi:10.3334/CDIAC/otg.CO2SYS_MATLAB_v1.1

Hirsh, H. K., K. J. Nickols, Y. Takeshita, S. B. Traiger, D. A. Mucciarone, S. Monismith, and R. B. Dunbar. 2020. Drivers of biogeochemical variability in a Central California kelp Forest: Implications for local amelioration of ocean acidification. J. Geophys. Res. Ocean. **125**: 1–22. doi:10.1029/2020JC016320

Hofmann, G. E., and and others. 2011. High-frequency dynamics of ocean pH: A multi-ecosystem comparison. PLoS One **6**: e28983. doi:10.1371/journal.pone.0028983

Jiang, Z., T. Tyrrell, D. J. Hydes, M. Dai, and S. E. Hartman. 2014. Variability of alkalinity and the alkalinity-salinity relationship in the tropical and subtropical surface ocean. Global Biogeochem. Cycles **28**: 729–742. doi:10.1002/2013GB004678

Li, X., M. I. García-Ibáñez, B. R. Carter, B. Chen, Q. Li, R. A. Easley, and W. J. Cai. 2020. Purified meta-cresol purple dye perturbation: How it influences spectrophotometric pH measurements. Mar. Chem. **225**: 103849. doi:10.1016/j.marchem.2020.103849

Liu, X., R. H. Byrne, M. Lindemuth, R. Easley, and J. T. Mathis. 2015. An automated procedure for laboratory and shipboard spectrophotometric measurements of seawater alkalinity: Continuously monitored single-step acid additions. Mar. Chem. **174**: 141–146. doi:10.1016/j.marchem.2015.06.008

Liu, X., M. C. Patsavas, and R. H. Byrne. 2011. Purification and characterization of meta-cresol purple for spectrophotometric seawater pH measurements. Environ. Sci. Technol. **45**: 4862–4868. doi:10.1021/es200665d

Ma, J., H. Shu, B. Yang, R. H. Byrne, and D. Yuan. 2019. Spectrophotometric determination of pH and carbonate ion concentrations in seawater: Choices, constraints and consequences. Anal. Chim. Acta **1081**: 18–31. doi:10.1016/j.aca.2019.06.024

Mosley, L. M., S. L. G. Husheer, and K. A. Hunter. 2004. Spectrophotometric pH measurement in estuaries using thymol blue and m-cresol purple. Mar. Chem. **91**: 175–186. doi:10.1016/j.marchem.2004.06.008

Müller, J. D., and G. Rehder. 2018. Metrology of pH measurements in brackish waters—Part 2: Experimental characterization of purified meta-cresol purple for spectrophotometric pHT measurements. Front. Mar. Sci. **5**: 1–9. doi:10.3389/fmars.2018.00177

Müller, J. D., B. Schneider, S. Aßmann, and G. Rehder. 2018. Spectrophotometric pH measurements in the presence of dissolved organic matter and hydrogen sulfide. Limnol. Oceanogr. Methods **16**: 68–82. doi:10.1002/lom3.10227

Newton, J. A., R. A. Feely, E. B. Jewett, P. Williamson & J. Mathis 2015. Global Ocean acidification observing network: Requirements and governance plan.

Patsavas, M. C., R. H. Byrne, and X. Liu. 2013. Purification of meta-cresol purple and cresol red by flash chromatography: Procedures for ensuring accurate spectrophotometric seawater pH measurements. Mar. Chem. **150**: 19–24. doi:10.1016/j.marchem.2013.01.004

Rérolle, V. M. C., C. F. A. Floquet, M. C. Mowlem, D. P. Connelly, E. P. Achterberg, and R. R. G. J. Bellerby. 2012. Seawater-pH measurements for ocean-acidification observations. TrAC Trends Anal. Chem. **40**: 146–157. doi:10.1016/j.trac.2012.07.016

Riebesell, U., V. J. Fabry, and J.-P. Gattuso [eds.]. 2010. Guide to best practices for ocean acidification research and data reporting. Publications Office of the European Union. https://op.europa.eu/en/publication-detail/-/publication/51887496-10b6-4b42-9876-1c2a1346fac5

Silbiger, N. J., and C. J. B. Sorte. 2018. Biophysical feedbacks mediate carbonate chemistry in coastal ecosystems across spatiotemporal gradients. Sci. Rep. **8**: 1–11. doi:10.1038/s41598-017-18736-6

Takeshita, Y., and and others. 2015. Including high-frequency variability in coastal ocean acidification projections. Biogeosciences **12**: 5853–5870. doi:10.5194/bg-12-5853-2015

Takeshita, Y., and and others. 2021a. Accurate pH and O2 measurements from spray underwater gliders. J. Atmos. Oceanic Tech. **38**: 181–195. doi:10.1175/JTECH-D-20-0095.1

Takeshita, Y., and and others. 2021b. Consistency and stability of purified meta-cresol purple for spectrophotometric pH measurements in seawater. Mar. Chem. **236**: 104018. doi:10.1016/j.marchem.2021.104018

Takeshita, Y., K. S. Johnson, T. R. Martz, J. N. Plant, and J. Sarmiento. 2018. Assessment of autonomous pH measurements for determining surface seawater partial pressure of CO2. J. Geophys. Res. Ocean. **123**: 4003–4013. doi:10.1029/2017JC013387

Takeshita, Y., W. McGillis, E. M. Briggs, A. L. Carter, E. M. Donham, T. R. Martz, N. N. Price, and J. E. Smith. 2016. Assessment of net community production and calcification of a coral reef using a boundary layer approach. J. Geophys. Res. Ocean. **121**: 5655–5671. doi:10.1002/2016JC011886

Williams, N. L., and and others. 2017. Calculating surface ocean pCO 2 from biogeochemical Argo floats equipped with pH: An uncertainty analysis. Global Biogeochem. Cycles **31**: 591–604. doi:10.1002/2016GB005541

Wright-Fairbanks, E. K., T. N. Miles, W. J. Cai, B. Chen, and G. K. Saba. 2020. Autonomous observation of seasonal carbonate chemistry dynamics in the mid-Atlantic bight. J. Geophys. Res. Ocean. **125**: e2020JC016505. doi:10.1029/2020JC016505

Yuan, S., and M. D. Degrandpre. 2008. Evaluation of indicator-based pH measurements for freshwater over a wide range of buffer intensities. Environ. Sci. Technol. **42**: 6092–6099. doi:10.1021/es800829x

Acknowledgments

This work was supported by the David and Lucile Packard Foundation and NSF OCE-1736864. The authors thank the William and Linda Frost Fund for supporting Addie Norgaard, Sara Gray, and Maddie Verburg as Frost Research Fellows through the Frost Undergraduate Student Research Award. They also thank the crew and science party of the Western Flyer for the C3PO cruise.

Submitted 02 December 2021
Accepted 24 February 2022

Associate editor: Gregory A. Cutter